

Designs for 25-kA and 40-kA Vapor-Cooled Bi2223/Copper Leads with the Bi2223 Section Operating in the Current-Sharing Mode

Haigun Lee*, Ho Min Kim*, Yukikazu Iwasa* and Keeman Kim**

Abstract - This paper presents reference designs for vapor-cooled HTS/Copper leads rated at 25 kA and 40 kA and that satisfy a protection criterion. Each HTS section is cooled by the effluent helium vapor boiling from a 4.2-K bath. Each HTS section is based on a design concept in which a short portion of its warm end (77.3 K) operates in the current-sharing mode; such operation results in a considerable saving for HTS materials required in the HTS section. Two designs of “fully superconducting” vapor-cooled HTS sections, one rated at 25 kA and the other at 40 kA are also presented as comparison bases for the new HTS sections. Each warm end of HTS sections is coupled to an optimal vapor-cooled copper lead rated at the same current as that for the HTS section. The extra coolant required at 77.3 K at the coupling station, an optimal length of the copper section will be shorter than that optimized for helium-vapor cooling between 4.2 K and room temperature.

Keywords: high-temperature superconducting (HTS) current lead

1. Introduction

A “large-scale” superconducting magnet, cooled in a bath of liquid helium, generally operates at a current in the range 5-50 kA. High-current vapor-cooled leads based entirely on copper are well established and readily purchasable from vendors. However, since the discovery of high-temperature superconductors (HTS) in the 1980s it has been agreed that replacing the cold section (4.2-77.3 K) of a vapor-cooled copper lead with an HTS section would substantially reduce the total heat input of the lead to the 4.2-K bath. Hull has classified altogether 11 types of lead configurations depending on how each HTS/normal-metal lead may be coupled [1].

In this paper we present reference designs for vapor-cooled copper/HTS leads rated at 25 kA and 40 kA, based on a design concept in which over a short length at the warm end of the HTS section is operated in the *current-sharing* mode [2-4]. The current-sharing mode operation of for our HTS sections, each comprised of paralleled Bi-2223/Ag-Au tape, results in a significant saving of the superconducting materials (Bi-2223/Ag-Au) needed to construct the HTS section compared with that of a HTS counterpart that operates fully superconducting over the entire HTS section.

Altogether eight designs are presented, four each for the two rate currents. Of the four designs at each rated current, the first is for a fully superconducting (*FullSu-*

per) version, presented here as a base line for the three remaining “current-sharing” (*CurShare*) versions. Also, for each rate current, the cold-end heat input, Q_{in} , of each of the three *CurShare* versions is set equal to that of the *FullSuper* counterpart. The required quantities of Bi-2223/Ag-Au for *CurShare* versions chosen for the study are ~70%, ~60%, and ~50% of the *FullSuper* version rated at the same current.

Strictly speaking, both LTS and HTS are dissipative when carrying a current, AC or even DC, albeit at rates much smaller than those for normal metal. Therefore, *all* HTS leads may be considered resistive. What distinguish our HTS lead from other HTS leads are: 1) design premise; and 2) degree of dissipation. Thus, our HTS section is deliberately designed to operate, though only over a small portion at the warm end, in the resistive mode with its Joule dissipation rate roughly of the same order as conduction heat flow from the warm end to the cold end, the sum of which is balanced by the effluent helium warming from 4.2 K to 77.3 K. In contrast, fully superconducting HTS sections dissipate Joule heat at most in the milliwatts range and the effluent helium devoted entirely to balance the conduction heat.

1.1 Basic Configuration

Fig. 1 shows a schematic drawing of the configuration of our vapor-cooled HTS/Copper lead that spans from 4.2 K (liquid helium) to room temperature (293 K). The lead is comprised of an HTS section which is coupled to a copper section at the 77.3 K station. As stated above, the HTS section comprises of paralleled Bi-2223/Ag-Au

* MIT Francis Bitter Magnet Laboratory (FBML), Cambridge, MA 02139, U.S.A. (hlee@jokaku.mit.edu)

** Nuclear Fusion R&D Center, Korea Basic Science Institute (KBSI), Korea (kkeeman@kbsi.re.kr)

Received July 2, 2003 ; Accepted August 25, 2003

tapes, each of active length l . The HTS section injects heat, Q_{in} , into liquid helium, generating effluent helium vapor, of mass flow rate \dot{m}_{he} , that absorbs over its temperature range, most of conduction heat and Joule dissipation generated in the current-sharing part of the HTS section.

Between T_l and room temperature, the HTS section rated at I_t is coupled to an optimal vapor-cooled copper section rated also at I_t . Because Q_{in} of the HTS section is necessarily smaller than that of an optimal vapor-cooled lead rated for the same rated I_t , the helium flow rate \dot{m}_{he} generated by the HTS section is insufficient for the Cu section. The extra coolant is thus introduced at the 77.3-K station, as indicated in Fig. 1. Note that an optimal vapor-cooled copper lead is designed to transport stably at a minimum LHe boiloff rate. The cold-end heat into the bath of an optimal vapor-cooled copper lead operating between 4.2 K and room temperature is $\sim 1\text{W/kA}$ or $\sim 25\text{W}$ for an optimal 25-kA copper lead and $\sim 40\text{W}$ for an optimal 40-kA vapor-cooled copper lead [5].

1.2 Unique Features of HTS Section

There are two unique features in our HTS section.

1) Its Q_{in} , the cold-end heat input, may be set either equal to or less than that of a *FullSuper* counterpart. Note that in either our or *FullSuper* version, Q_{in} can be set at a fraction of that for an optimal vapor-cooled copper lead of the same rated current.

2) If desirable the quantity of Bi-2223/Ag-Au tape may be selected to be a fraction of its *FullSuper* counterpart.

2. Reference Design for 25-kA and 40-kA HTS Sections

The design procedure for four versions each of 25-kA and 40-kA leads, a *FullSuper* and three *CurShare* versions, 1-3, are described first.

2.1 Design Procedure-Iteration 1

Given below is a step-by-step procedure for design of the four HTS sections. In Iteration 1, a protection criterion is not included in the design; it will be included in Iteration 2.

Step 1: Parameters of Bi-2223/Ag-Au Tape Key parameters of Bi-2223/Ag-Au tape are: 1) overall dimensions: width; thickness; and Bi-2223 filling (volume, in %); 2) critical currents in self field: $i_c(T_l)$ and $i_c(T_0)$,

3) Ag-Au alloy: Au content; cross sectional area, a_m ; T -averaged thermal conductivity, \tilde{k}_m , in the range $T_0 - T_l$; these parameters of Bi-2223/Ag-Au tape manufactured by and T -averaged electrical resistivity, $\tilde{\rho}_m$. Table 1 presents American Superconductor Corp. (AmSC).

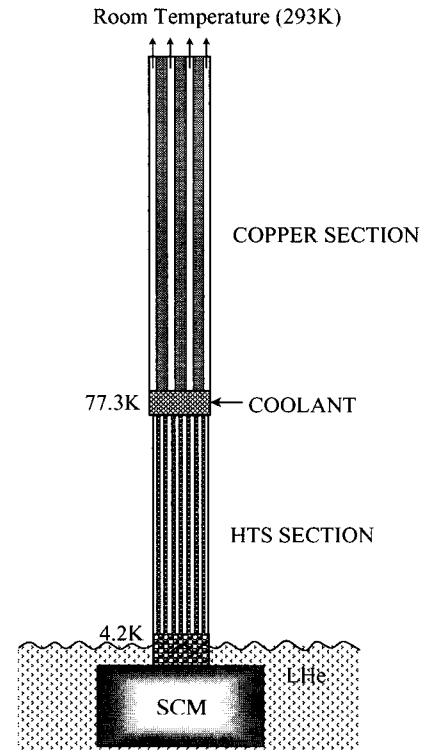


Fig. 1 Schematic drawing of a vapor-cooled HTS / Copper lead with HTS Section couple at 77.3 K to Copper Section.

Table 1 Parameters of AMSC Bi-2223/Ag-Au Tape

Parameters		Value
Overall width	[mm]	4.064
Overall thickness	[mm]	0.203
Bi-2223 filling (volume)	[%]	42
Au content	[wt%]	5.3
Ag-Au cross section, a_m	[mm ²]	0.479
{ a_{tp} (tape cross section) }	[mm ²]	0.825
$i_c(T_l)$ (@77.3 K @B _⊥ = 0.2 T)	[A]	100*
$i_c(T_0)$ (@4.2 K @B _⊥ = 0.2 T)	[A]	500†
\tilde{k}_m (4.2~77 K)	[W/cm K]	0.327
$\tilde{\rho}_m$ (4.2~77 K)	[μΩcm]	1.0

* 1-μV/cm criterion. † Estimated.

Step 2: Bi-2223/Ag-Au Quantity Because $I_c(T_l) = N_{tp}i_c(T_l)$, where $I_c(T_l)$ is the critical current at the warm end and N_{tp} is the number of paralleled tapes and $i_c(T_l) = 100$ A, values of N_{tp} are 250 (25 kA) and 400 (40 kA) for *FullSuper* versions. For *CurShare* Versions

1-3, N_{tp} 's are, respectively, 70%, 60%, and 50% of 250 and 400.

Step 3: Current-Sharing Temperature Once $i_c(T_l)$ is selected, the current-sharing temperature, T_{cs} , may be determined. For this, it is assumed that $I_c(T) \equiv N_{tp} i_c(T)$ is a linear function of T , decreasing linearly from $I_c(T_0) = N_{tp} i_c(T_0)$ to $i_c(T_l)$. From this linear function, we may determine T_{cs} , at which point $I_t = I_c(T_{cs})$.

Step 4: Design of FullSuper Version First, design a *FullSuper* counterpart for a given combination of Q_{in} and l , which are related by:[3,4]

$$Q_{in} = \frac{\tilde{k}_m A_m h_L}{\tilde{C}_p l} \ln \left[\frac{\tilde{C}_p (T_l - T_0)}{h_L} + 1 \right] \quad (1)$$

In Eq. 1 A_m is the total cross sectional area of the Ag-Au alloy, given by $A_m = N_{tp} a_m$. Note that by definition $N_p = I_t / i_c(T_l)$, because the *FullSuper* HTS section, carrying I_t , is superconducting even at the warm end (T_l). For rated current of 25 kA and 40 kA, because $i_c(T_l) = 100$ A, values of N_{tp} are, respectively, 250 and 400.

With $h_L = 20.4$ J/g (liquid helium at 4.2 K); $\tilde{C}_p = 5.280$ J/g·K (helium vapor, 4.2~80 K); $T_0 = 4.2$ K; and $T_l = 77.3$ K, a value Q_{in} of may be computed from Eq. 1 for a given choice of l . For $l = 20$ cm: $Q_{in} = 0.199$ W for 25 kA and 0.319 W for 40 kA. Because standard America Magnet Inc. (AMI) vapor-cooled copper leads rated 25 kA and 40 kA have Q_{in} values, respectively, of ~30W and ~48 W, the corresponding HTS/Copper leads reduce Q_{in} from those of the copper leads by a factor more than 100.

Step 5: Protection Criterion Before proceeding further, it is appropriate at this point to introduce a protection criterion in the design. Here we review a fault-mode scenario for protection of a vapor-cooled current lead: flow stoppage.

We may analyze this condition by assuming the adiabatic condition in which Joule heating is converted to raising the lead temperature: [5]

$$\rho_m(T) J_m^2(t) = C_{tp}(T) \frac{dT_m(t)}{dt} \quad (2)$$

where $\rho_m(T)$ and $J_m(t)$ are, respectively, the resistivity and current density of the matrix; $C_{tp}(T)$ is the heat capacity of the tape (Bi-2223 and Ag-Au); and $T_m(t)$ is the matrix temperature. Based on the assumption that $C_{bi2223}(T) \approx C_{agau}(T)$, with the 58%/42% = 1.38 to take

into account the volumetric ratio of this tape, we may assume $C_{tp}(T) \approx 1.38 C_m(T)$ and integrate Eq. 2 in time and temperature as given below:

$$\int J_m^2(t) dt \equiv 1.38 \int_{T_i}^{T_f} \frac{C_m(T)}{\rho_m(T)} dT \equiv 1.38 \frac{\Delta H_m(T_i, T_f)}{\rho_m} \quad (3)$$

where $\Delta H_m(T_i, T_f)$ is the total change in enthalpy of the matrix between T_i and T_f . The second approximation of Eq. 3 is valid for alloys whose resistivity is nearly constant over this temperature span. The left-hand side of Eq. 3 may be divided into two time segments, first between $t = 0$ (start of flow stoppage) and $t = \tau_{del}$ (delay in discharge action), and second between $t = \tau_{del}$ and $t = \tau_{del} + \tau_{dis}$, where τ_{dis} is the exponential discharge time constant. From Eq. 3, we may derive a protection criterion for an HTS section:

$$J_{mo}^2 \tau_{del} + \frac{1}{2} J_{mo}^2 \tau_{dis} \leq 1.38 \frac{\Delta H_m(T_i, T_f)}{\tilde{\rho}_m} \quad (4)$$

where $J_{mo} \equiv I_t / A_m$ is the matrix current density in at $t = 0$.

We apply Eq. 4 to the *FullSuper* HTS section, which for $A_m = 250 a_m = 1.20$ cm² (25 kA) and $A_m = 400 a_m = 1.92$ cm² (40 kA) has a value of $J_{mo} = 20.83$ kA/cm². The left-hand side of Eq. 4, for $\tau_{del} = 5$ s and $\tau_{dis} = 15$ s, for example, is thus 54.2×10^8 A² s/cm⁴.

With $T_i = 77$ K, $T_f = 200$ K, and $\tilde{\rho}_m = 1 \times 10^{-6}$ Ωcm, the right-hand side of Eq. 4 is 3.6×10^8 A²·s/cm⁴ for the enthalpy and density of silver. Clearly, the protection criterion of Eq. 4 is not met even by the *FullSuper* version, rated at 25 kA and 40 kA. This obviously implies none of *CurShare* versions 1-3 would meet the protection criterion.

2.2 Design Procedure – Iteration 2

Step 0: Parameters of Bi-2223/Ag-Au Tape The parameters of Bi-2223/Ag-Au tape are identical to those in the Iteration 1 design given in Table 1.

Step 1: Protection Requirement—Left-Hand Side of Eq. 4 Because even the total matrix cross sectional area of 1.20 cm² (25 kA) and 1.92 cm² (40 kA) for the *FullSuper* HTS section are utterly inadequate to satisfy the condition of Eq. 4, it is necessary to introduce in each HTS section an additional normal metal (NM) element, thereby to reduce J_{mo} . The total NM cross section area, A_{nm} , may be determined from Eq. 4. By neglecting A_m , we may express the left-hand side of Eq. 4 as:

$$\left(\frac{I_t}{A_{nm}}\right)^2 \tau_{del} + \frac{1}{2} \left(\frac{I_t}{A_{nm}}\right)^2 \tau_{dis} = \left(\frac{I_t}{A_{nm}}\right)^2 \left(\tau_{del} + \frac{1}{2} \tau_{dis}\right) \quad (5)$$

Right-Hand Side of Eq. 3 This normal metal must have the following properties.

1) Low T -averaged electrical resistivity, $\tilde{\rho}_{nm}$. Note that a low value of $\tilde{\rho}_{nm}$ will enhance the right-hand side of Eq. 4.

2) Low T -averaged thermal conductivity, \tilde{k}_{nm} . Note that \tilde{k}_{nm} will appear in a new expression for Q_{in} similar to Eq. 1.

3) Common material and readily available in tape form.
4) Easily solderable to Bi-2223/Ag-Au tape.

A potential candidate for this metal is brass, key properties of which are as follows.

1) $\tilde{\rho}_{nm} = 2.84 \times 10^{-6} \Omega\text{cm}$ in the range 77-200 K; $2.25 \times 10^{-6} \Omega\text{cm}$ (4.2-77 K) [4].

2) $\tilde{k}_{nm} = 0.35 \text{ W/K}\cdot\text{cm}$ in the range 4.2-77 K.

Approximating brass (Cu-Zn) as copper, we obtain for $T_i = 77 \text{ K}$ and $T_f = 200 \text{ K}$:

$$\left(\frac{I_t}{A_{nm}}\right)^2 \left(\tau_{del} + \frac{1}{2} \tau_{dis}\right) \leq 1.14 \times 10^8 [A^2 s / \text{cm}^4] \quad (6)$$

With $\tau_{del} = 5 \text{ s}$ and $\tau_{dis} = 15 \text{ s}$: $A_{nm} = 8.28 \text{ cm}^2$ for 25-kA and 13.25 cm^2 for 40 kA lead. These are also applicable to CurShare versions 1-3.

Step 2: Bi-2223/Ag-Au Quantity The numbers of tapes in a *FullSuper* version and the new 6-kA leads are the same as those of the Iteration 1 design.

Configuration Because this extra NM element required by protection should also be vapor-cooled and because Bi-2223/Ag-Au is in the form of paralleled tapes, this too should be in the form of paralleled tapes, each NM tape soldered preferably soldered to each superconductor (SC) tape to enhance heat exchange performance.

Dimensions of NM Tape A thickness of 0.508 mm is chosen for each NM tape. The width, same for 25-kA and 40-kA sections, varies according to N_{tp} and A_{nm} .

For *FullSuper* versions it is 16.3 mm for both 25 kA and 40 kA; for *CurShare* versions 1-3, they are, respectively, 23.3, 27.2, and 32.6 mm.

Step 3: Current-Sharing Temperature This step is identical to that in Iteration 1. For *CurShare* versions 1-3, values of T_{cs} are, respectively, 72.2, 65.1, and 59.0 K, for 25 kA and 40 kA sections. For the *FullSuper* versions, a value of 77.3 K may be assigned, implying, by definition, existence of no current-sharing region in the *FullSuper*

versions.

Step 4: FullSuper Version With this normal metal included, Eq. 1 is modified to:

$$Q_{in} = \frac{(\tilde{k}_m A_m + \tilde{k}_{nm} A_{nm}) h_L}{\tilde{C}_P l} \ln \left[\frac{\tilde{C}_P (T_l - T_0)}{h_L} + 1 \right] \quad (7)$$

Equation 7 gives: $Q_{in} = 1.90 \text{ W}$ for 25 kA and 3.04 W for 40-kA, nearly 10 times greater than those computed in the Iteration 1 design. The new values of Q_{in} are still less than 1/10 those of corresponding AMI standard vapor-cooled copper leads.

Step 5: Current-Sharing Regime The current sharing regime spans from $z = l_{cs}$ to $z = l$ (T_0 is at $z = 0$ and T_l at $z = l$). Normalized to l , z becomes ξ , l to 1, and l_{cs} to ξ_{cs} . As detailed in earlier papers [3,4], ξ_{cs} may be determined by satisfying the following equation, in which the only unknown is ξ_{cs} for a given set of α_{cs} and β_{cs} defined below:

$$e^{\frac{\alpha_{cs}}{2\xi_{cs}}} \sin \left[\frac{\beta_{cs} (1 - \xi_{cs})}{\xi_{cs}} \right] = \frac{\beta_{cs} (e^{\alpha_{cs}} - 1) (T_l - T_{cs})}{\alpha_{cs} e^{\frac{\alpha_{cs}}{2}} (T_{cs} - T_0)} \quad (8)$$

where

$$\alpha_{cs} \equiv \frac{\dot{m}_{he} \tilde{C}_P l_{cs}}{(\tilde{k}_m A_m + \tilde{k}_{nm} A_{nm})} = \ln \left[\frac{\tilde{C}_P (T_{cs} - T_0)}{h_L} + 1 \right] \quad (9)$$

Because of the presence of the normal metal element, β_{cs} is modified [3,4]:

$$\beta_{cs} = \sqrt{\frac{\tilde{\rho}_{nm} \tilde{\rho}_{mt} (l - l_{cs})}{(\tilde{k}_m A_m + \tilde{k}_{nm} A_{nm}) (\tilde{\rho}_m A_m + \tilde{\rho}_{nm} A_{nm}) (T_l - T_{cs})}} \frac{1}{4} \left(\frac{\dot{m}_{he} \tilde{C}_P}{\tilde{k}_m A_m + \tilde{k}_{nm} A_{nm}} \right)^2 \quad (10)$$

Step 6: HTS Section Length The total HTS section length, l , may be given by $l = l_{cs} / \xi_{cs}$, where ξ_{cs} is determined from Eq. 8 and l_{cs} is determined from the first expression of Eq. 9 for a given value of \dot{m}_{he} , which is equal to Q_{in} / h_L .

Step 7: Heat Exchange Requirements Stable operation of a vapor-cooled lead, HTS section or copper section, is possible only when the total required cooling power is properly heat-exchanged with the active element of the lead. One parameter that can gauge heat exchange performance is an effective cooling flux, q_{ef} , in the lead. q_{ef} may be given by the total cooling power divided by the total surface area of the element exposed to cooling. Based on performance of standard AMI vapor-cooled copper leads, q_{ef} values 100 mW/cm² or less are considered adequate [7].

Table 2: 25-kA & 40-kA HTS Sections-Iteration 2

25-κA		<i>FullSuper</i>	<i>CurShare 1</i>	<i>CurShare 2</i>	<i>CurShare 3</i>
# tapes, SC & NM (N_{tp})		250	175	150	125
$I_c(T_l)$ (@77.3K)	[kA]	25	17.5	15	12.5
Ag-Au area, A_m	[cm ²]	1.20	0.84	0.72	0.60
Q_{in}	[W]	1.90			
NM tape area, A_{nm}	[cm ²]	8.28			
40-κA		<i>FullSuper</i>	<i>CurShare 1</i>	<i>CurShare 2</i>	<i>CurShare 3</i>
# tapes, SC & NM (N_{tp})		400	280	240	200
$I_c(T_l)$ (@77.3K)	[kA]	40	28	24	20
Ag-Au area, A_m	[cm ²]	1.92	1.34	1.15	0.96
Q_{in}	[W]	3.04			
NM tape area, A_{nm}	[cm ²]	13.25			
25-κA & 40-κA		<i>FullSuper</i>	<i>CurShare 1</i>	<i>CurShare 2</i>	<i>CurShare 3</i>
T_{cs}	[K]	77.3	72.2	65.1	59.0
l	[cm]	200	193	191	188
$l-l_{cs}$	[mm]	0	4.4	11	17
$\rho_m; \rho_{nm}$	[μΩcm]	1.0 ; 2.25			
$k_m; k_{nm}$	[W/Kcm]	0.327 ; 0.35			
NM tape width	[mm]	6.5	9.3	10.9	13.0
Cooling flux	[mW/cm ²]	11	11	12	12
Required HTS tape		1	0.68	0.57	0.47

† For tape thickness of 0.508 mm. ‡ Normalized to *FullSuper*.

For each HTS section, q_{ef} may be given by:

$$q_{ef} = \frac{\dot{m}_{he} \tilde{C}_p (T_l - T_0)}{N_{tp} l w_{nm}} \quad (11)$$

where w_{nm} is the NM tape width. In Eq. 11, it is assumed, to enhance heat exchange (or to reduce q_{ef}), that each superconductor (SC) tape is soldered to an NM tape; each NM tape may thus be regarded as a fin to the SC tape.

Note that in Eq. 11, to be conservative, $N_{tp} l w_{nm}$, which represents one *half* of the total surface of NM tapes theoretically exposed to the cooling vapor, is used to compute q_{ef} . For each of four versions (25 kA or 40 kA), the values of q_{ef} computed, 11-12 mW/cm², are well below ~100 mW/cm². If q_{ef} values turn out to be greater than ~100 mW/cm², then it may require another iteration process.

Table 2 presents key parameters of 25-kA and 40-kA HTS sections based on the Iteration 2 design: *FullSuper* in Column 2; *CurShare* versions 1-3, respectively, Columns 3-5. The table shows that the amount of HTS tape required by the *CurShare* versions 1-3, for the same Q_{in} as that of the *FullSuper* versions, are 68 %, 57 %, and 47 % of those required by the *FullSuper* versions.

As inferred from the table, tape length becomes shorter

as N_{tp} is reduced – more saving of SC is possible. Because q_{ef} is essentially determined by A_{nm} , which in turn is dictated by protection requirements, it is possible to reduce N_{tp} even further than 50 % without violating either protection or heat-exchange requirements.

3. Copper Section

For the copper section we begin by choosing standard AMI vapor-cooled leads, one rated at 25 kA and the other rated at 40 kA, each with a specific combination of active area, A_{cu} , and length, l_{cu} with the ratio $I_t l_{cu} / A_{cu}$ optimized for use with the cold end extended to liquid helium temperature. We then proceed to determine a required cooling flow rate and consider if each lead can meet protection and heat exchange requirements. For a coolant to be introduced at the cold end of the copper section at 77 K, which is the cold-end temperature used in this analysis, there are three choices: 1) gaseous helium; 2) gaseous nitrogen; and 3) liquid nitrogen.

The objective here is to determine an appropriate value of mass flow rate, \dot{m}_f , for a given coolant. Let us use a standard AMI 25-kA lead as an example to estimate mass

flow rates for the three coolants. Note that this lead has $Q_{in} \approx 30$ W at the 4.2-K cold end, which, when divided by $h_L = 20.4$ J/g, gives $\dot{m}_{he} \approx 1.5$ g/s.

Gaseous Helium If 77-K helium gas is introduced at the cold-end of the copper lead, its mass flow rate, \dot{m}_{fl} , must obviously be equal to $\dot{m}_{he} : \dot{m}_{fl} \approx 1.5$ g/s. Note that between 77 K and 293 K, this flow rate generates a total cooling power, $Q_{he} = \dot{m}_{he} \tilde{C}_p (293K - 77K) \approx 1708$ W.

Gaseous Nitrogen If 77-K nitrogen gas is introduced at the cold-end, its mass flow rate must give the same total cooling power between 77 K and 293 K as the helium gas. With nitrogen average specific heat, $\tilde{C}_{fl} = 1.042$ J/gK: $\dot{m}_{fl} \approx 7.59$ g/s.

Nitrogen Liquid Because liquid nitrogen's latent heat of vaporization is 199.3 J/g, its contribution is included in the cooling power and we have: $\dot{m}_{fl} \approx 4.0$ g/s.

3.1 Coolant Fluid Flow Rate

To better understand the thermal behavior of the copper section, we present here results of an analysis performed on two standard AMI vapor-cooled 25-kA and 40-kA copper leads selected for the copper sections of our integrated HTS/Copper leads. The analysis is divided into two parts: 1) gaseous coolants (helium or nitrogen); and 2) liquid nitrogen.

These leads have the following values of A_{cu} and l_{cu} : 8.58 cm² and 66.0 cm for 25-kA lead; 13.73 cm² and 66.0 cm for 40-kA lead [7].

Gas For a copper lead the following value of I_t and cooled with fluid mass flow rate, \dot{m}_{fl} , an expression of the steady state ($dT/dt=0$) power density equation may be given by:

$$\tilde{k}_{cu} A_{cu} \frac{d^2 T}{dz^2} - \dot{m}_{fl} \tilde{C}_{fl} \frac{dT}{dz} + \frac{I_t^2 \gamma_{cu}}{A_{cu}} (T - T_0) + \frac{I_t^2 \rho_0}{A_{cu}} = 0 \quad (12)$$

In Eq. 12, \tilde{k}_{cu} is the T-averaged copper thermal conductivity (77-293 K); \tilde{C}_{fl} is the fluid T-averaged specific heat; γ_{cu} and ρ_0 are, respectively, the resistivity temperature coefficient and resistivity at T_0 is the cold-end temperature, set at 77 K for this analysis. Although Eq. 12 is solvable in closed form, because over most of the 77-293 K range the last term in the left-hand side of Eq. 12 is negligible compared with the third term, we shall neglect it here in order to obtain simpler closed-form expressions. Thus:

$$\tilde{k}_{cu} A_{cu} \frac{d^2 T}{dz^2} - \dot{m}_{fl} \tilde{C}_{fl} \frac{dT}{dz} + \frac{I_t^2 \gamma_{cu}}{A_{cu}} (T - T_0) \equiv 0 \quad (13)$$

With a boundary condition of $T = T_l$ at $z = l_{cu}$, $\theta(z) \equiv T(z) - T_0$ may be given by:

$$\theta(z) = \frac{\theta_{l_{cu}}}{e^{\alpha_{cu} l_{cu}} \sin(\beta_{cu} l_{cu})} e^{\alpha_{cu} z} \sin(\beta_{cu} z) \quad (14)$$

where

$$\alpha_{cu} = \frac{\dot{m}_{fl} \tilde{C}_{fl}}{2 \tilde{k}_{cu} A_{cu}} \quad (15a)$$

$$\beta_{cu} = \sqrt{\frac{I_t^2 \gamma_{cu}}{\tilde{k}_{cu} A_{cu}^2} - \left(\frac{\dot{m}_{fl} \tilde{C}_{fl}}{2 \tilde{k}_{cu} A_{cu}} \right)^2} \quad (15b)$$

We may force θ_{max} to occur at $z = l_{cu}$ by setting $d\theta/dz = 0$ and obtain:

$$\frac{1}{2} \dot{m}_{fl} \tilde{C}_{fl} + \tilde{k}_{cu} A_{cu} \beta_{cu} \cot(\beta_{cu} l_{cu}) = 0 \quad (16)$$

For a given set of parameters, i.e., A_{cu} , l_{cu} , I_t , \tilde{C}_{fl} , γ_{cu} , there is a unique value of \dot{m}_{fl} that satisfies Eq. 16. Note that because the $\cot(\beta_{cu} l_{cu})$ becomes negative in the range 90-180°, θ_{max} occurs not at $\beta_{cu} l_{cu} = \pi/2$, as Eq. 14 may imply, but beyond $\pi/2$.

Conduction Heat & Joule Dissipation The cold-end heat input, Q_0 , is given by:

$$Q_0 = \tilde{k}_{cu} A_{cu} \left. \frac{d\theta(z)}{dz} \right|_{z=0} = \frac{\tilde{k}_{cu} A_{cu} \theta_{l_{cu}} \beta_{cu}}{e^{(\alpha_{cu} l_{cu})} \sin(\beta_{cu} l_{cu})} \equiv 0 \quad (17)$$

$Q_0 \equiv 0$ because of a large exponential term—due to $l_{cu} = 66$ cm—in the denominator and a small value of β_{cu} in the numerator. This will be shown numerically later.

The warm-end conduction heat, $Q_{l_{cu}}$ is, by definition, zero (Eq. 16). That is, because no heat enters or leaves the lead by conduction from either end, the coolant is used entirely to remove the Joule dissipation, Q_j , generated in the lead, which is given by:

$$Q_j = \frac{I_t^2 \gamma_{cu}}{A_{cu}} \int_0^{l_{cu}} \theta(z) dz \quad (18)$$

Combining Eqs. 14 and 18, we obtain:

$$\begin{aligned}
 Q_j &= \frac{I_1^2 \gamma_{cu} \theta_{l_{cu}}}{A_{cu} e^{\alpha_{cu} l_{cu}} \sin(\beta_{cu} l_{cu})} \int_0^{l_{cu}} e^{\alpha_{cu} z} \sin(\beta_{cu} z) dz \\
 &= \frac{I_1^2 \gamma_{cu} \theta_{l_{cu}}}{A_{cu} (\alpha_{cu}^2 + \beta_{cu}^2)} \left[\frac{\dot{m}_{fl} \tilde{C}_{fl}}{2 \tilde{k}_{cu} A_{cu}} - \beta_{cu} \cot(\beta_{cu} l_{cu}) \right] \\
 &+ (\text{terms containing } e^{-\alpha_{cu} l_{cu}}) \\
 &\cong \tilde{k}_{cu} A_{cu} \theta_{l_{cu}} \left[\frac{\dot{m}_{fl} \tilde{C}_{fl}}{2 \tilde{k}_{cu} A_{cu}} - \beta_{cu} \cot(\beta_{cu} l_{cu}) \right] \\
 &= \frac{1}{2} \dot{m}_{fl} \tilde{C}_{fl} \theta_{l_{cu}} - \tilde{k}_{cu} A_{cu} \theta_{l_{cu}} \beta_{cu} \cot(\beta_{cu} l_{cu}) \quad (19)
 \end{aligned}$$

\dot{m}_{fl} (Eq. 16) and Q_j (Eq. 19) may be computed for the 25-kA and 40-kA leads with the following parameter values: $\tilde{k}_{cu} = 4$ W/cm K; $\gamma_{cu} = 0.903 \times 10^{-8}$ Ω cm/K; $\tilde{C}_{fl} = 1.042$ J/g K (nitrogen) or 5.280 J/g K (helium).

Mass Flow Rate for 25-kA Lead After a few trials and errors, we find a cotangent angle of 159.75° to satisfy Eq. 16, with $\cot(\beta_{cu} l_{cu}) = -2.7077$ and $\beta_{cu} l_{cu} = 2.7878$. Thus:

$$l_{cu} \sqrt{\frac{I_1^2 \gamma_{cu}}{\tilde{k}_{cu} A_{cu}^2} - \left(\frac{\dot{m}_{fl} \tilde{C}_{fl}}{2 \tilde{k}_{cu} A_{cu}} \right)^2} = 2.7878 \quad (20)$$

From Eq. 20, we obtain: $\dot{m}_{fl} = 7.532$ g/s for nitrogen and 1.486 g/s for helium, each entering the cold end and as vapor at 77 K and exiting the warm end at 293 K ($\theta_{l_{cu}} = 216$ K).

$\dot{m}_{fl} = 7.532$ g/s must also satisfy Eq. 16. With $\beta_{cu} l_{cu} = 2.7878$ and $\cot(\beta_{cu} l_{cu}) = -2.7007$: $\dot{m}_{fl} = 7.534$ g/s from Eq. 16, which agrees well with 7.532 g/s computed from Eq. 20. Equations 16 and 20 thus give a self consistent value of \dot{m}_{fl} . Note that mass rates of 7.53 g/s and 1.49 g/s computed, respectively, for nitrogen and helium agree well with 7.59 g/s and 1.5 g/s estimated at the outset.

Joule Dissipation Inserting appropriate parameter values into Eq. 19, we obtain: $Q_j = 1696$ W, which agrees well with $Q_{fl} = \dot{m}_{fl} \tilde{C}_{fl} \theta_{l_{cu}} = 1695$ W, nitrogen or helium. That is, everything, as it must, is consistent.

As noted above in reference to Eq. 17, $Q_0 \cong 0$ because of the experimental term, $e^{\alpha_{cu} l_{cu}}$, and β_{cu} . For $\dot{m}_{fl} = 7.53$ g/s, we have, from Eq. 15a, $\alpha_{cu} = 0.1143$ cm^{-1} , which for $l_{cu} = 66$ cm gives $e^{\alpha_{cu} l_{cu}} = 1890$. Combined with $\beta_{cu} = 0.04224$ cm^{-1} and $\sin(\beta_{cu} l_{cu}) = 0.3464$, we

obtain: $Q_0 = 0.48$ W, which is indeed negligible.

Liquid Nitrogen When 77-K liquid nitrogen is introduced at the cold end at a mass flow rate of \dot{m}_{fl} , it generates a cooling power, $Q_{n2} = \dot{m}_{fl} h_{n2}$, at the cold end, where $h_{n2} = 199.3$ J/g is the heat of vaporization of the liquid at 77 K.

When a vapor-cooled copper lead is operated down to the liquid helium environment, as is usually the case, Q_{in} (heat input at 4.2 K) is matched by $\dot{m}_{fl} h_L$, where $h_L = 20.4$ J/g is the liquid helium heat of vaporization. A mass flow rate of the helium vapor thus generated is sufficient to keep the entire lead in stable condition. Because h_{n2} is nearly 10 times greater than h_L and more importantly because $Q_0 \cong 0$, as our example above illustrates, the cooling power of $\dot{m}_{fl} h_{n2}$ cannot be matched at the cold end.

What actually happens is that $\dot{m}_{fl} h_{n2}$ would be used to soak up the Joule heat generated over the lower portion of the lead, from the cold end to a distance of l_{lq} . This extended 77-K portion of the lead, because it is resistive, generates Joule heating Q_{jlq} , which is matched by $\dot{m}_{fl} h_{n2}$. Noting that the last term in the left-hand side of Eq. 12, neglected in the above, cannot be neglected at 77 K, we have:

$$Q_{jlq} = \frac{\rho_0 I_1^2 l_{lq}}{A_{cu}} = \dot{m}_{fl} h_{n2} \quad (21)$$

where $\rho_0 = 0.22 \times 10^{-6}$ Ω cm. In Eq. 21, l_{lq} and \dot{m}_{fl} are still unknown values.

With the lower portion of the lead, from $z=0$ to $z=l_{lq}$, kept at 77 K, the effective active (vapor-cooled) length of the lead becomes shorter: $l_{cu} - l_{lq}$ and Eq. 16 thus becomes:

$$\frac{1}{2} \dot{m}_{fl} \tilde{C}_{fl} + \tilde{k}_{cu} A_{cu} \beta_{cu} \cot[\beta_{cu} (l_{cu} - l_{lq})] = 0 \quad (22)$$

There is a unique combination of \dot{m}_{fl} and l_{lq} that satisfies both Eqs. 21 and 22.

Mass Flow Rate for 25-kA Lead For our 25-kA copper lead, a combination of $\dot{m}_{fl} = 3.75$ g/s and $l_{lq} = 46.64$ cm gives a unique solution to Eqs. 21 and 22. That is, only the top 19.36-cm long portion of the lead remains dry and vapor-cooled. Note that a mass rate of 4 g/s estimated at the outset agrees quite well with the computed rate.

The result implies that if only vapor (N_2 or He) is to be used as a coolant, a copper lead with the same A_{cu} and

an active length of 19.36 cm would not only operate stably but require \dot{m}_{fl} of only 3.75 g/s rather than 7.53 g/s computed above for the 66.0-cm lead.

Joule Dissipation in Dry Portion The 19.36-cm long portion of the lead remains dry and its total Joule dissipation, Q_j , must be equal to the total cooling power provided by the vapor: $\dot{m}_{fl}\tilde{C}_{fl}\theta_l=844.0$ W. For an active length of $l_{cu}-l_{lq}$, Eq. 19 becomes:

$$Q_j = \frac{1}{2}\dot{m}_{fl}\tilde{C}_{fl}\theta_{l_{cu}} - \tilde{k}_{cu}A_{cu}\theta_{l_{cu}}\beta_{cu}\cot[\beta_{cu}(l_{cu}-l_{lq})] \quad (23)$$

Equation 23 gives $Q_j=843.6$ W, which agrees well with a cooling power of 844.0 W.

Table 3 Parameters of Copper Leads

		25 kA	40 kA
Operating range	[K]	77-293	
Active area, A_{cu}	[cm ²]	8.58	13.73
Active length, l_{cu}	[cm]	66	
Cooling area*	[cm ²]	151,000	242,000
Cooling Mass Flow Rate			
N2 vapor, \dot{m}_{fl}	[g/s]	7.53	12.05
He vapor, \dot{m}_{fl}	[g/s]	1.49	2.38
$\dot{m}_{fl}\tilde{C}_{fl}\theta_l$	[W]	1950	3120
N2 liquid, \dot{m}_{fl}	[g/s]	3.75	6.0
$\dot{m}_{fl}\tilde{C}_{fl}\theta_l$	[W]	844	1350
Effective Heat Flux			
Vapor, q_{ef}	[mW/cm ²]	13	
Liquid, q_{ef}	[mW/cm ²]	19†	

4. Protection of Copper Lead

The Protection criterion of Eq. 6 with an appropriate value for its right-hand side may be used for these copper sections. Because the warm end is operated at 293 K, its fault-mode temperature should be limited to ~373 K. For copper, regardless of its impurity content, the right-hand side of Eq. 6 between 293 K and 373 K is $\sim 10^8$ A²s/cm⁴ [5]. Thus:

$$\left(\frac{I_t}{A_{cu}}\right)^2\left(\tau_{del} + \frac{1}{2}\tau_{dis}\right) \leq 1 \times 10^8 [A^2s/cm^4] \quad (24)$$

with $I_t = 25$ kA and $A_{cu} = 8.58$ cm², the left-hand side becomes 1.06×10^8 A²s/cm⁴—a combination of $I_t = 40$ kA and $A_{cu} = 13.73$ cm² gives the same value. That is, Eq. 24 is nearly satisfied. Because this criterion is quite conservative, we may conclude that the protection criterion is met for both rated currents.

4.1 Heat Exchange Performance

As with HTS sections, q_{ef} is computed for each lead: q_{ef} values are below 100 mW/cm². Table 3 presents key parameters of our 25-kA and 40-kA copper leads.

4.2 Remarks on Copper Section

As the thermal analysis presented above has shown, our choice of standard AMI vapor-cooled copper leads, rated 25-kA and 40-kA, are not necessarily optimized for copper sections of our vapor-cooled HTS/Copper leads. Namely, a vapor-cooled copper lead with the ratio $I_t l_{cu} / A_{cu}$ optimized for operation in the range 4.2-293 K is not necessarily optimized for use in the range 77-293 K. The analysis further demonstrates that the lead parameters depend on coolant type of vapor, nitrogen and helium, in terms of thermal performance there is no distinctive advantage of one over the other. However, because these leads are designed for vapor cooling, liquid cooling, particularly over a relatively long distance as has been shown to be the case in our 25-kA (and 40-kA) leads, may not be suitable: the fluid in this region, by necessity, will be in two phases, and a resultant pressure may prove to be too excessive for a required level of \dot{m}_{fl} .

5. Conclusions

Reference designs are presented for 25-kA and 40-kA vapor-cooled HTS/copper leads operating in the range 4.2-293 K. As demonstrated by these reference designs, each HTS section, based on a design concept in which a short portion of its warm end (77.3 K) operates in the current-sharing mode, requires HTS counterparts. The extra coolant flow rates required at the HTS-copper coupling station to provide sufficient cooling are computed for 25 kA and 40 ka copper sections. Our thermal analysis shows that if liquid nitrogen is introduced at 77 K at the coupling station, an optimal length of the copper section will be shorter than that optimized for helium-vapor cooling between 4.2 K and room temperature. Summarized below are key results for both HTS and copper sections.

HTS Section The design procedures for HTS sections, based on a thorough analysis, may be used to determine key parameters of an HTS section that meet specific requirements for a given rated current, the most important of which include: $Q_{in}; I_t$; and protection.

Copper Section Another analysis presented here for the copper section may be used to design an optimal copper section that meets specific requirements. Here important parameters are: l_{cu} ; T_0 (assumed 77 K in the analy-

sis); coolant (vapor or liquid nitrogen).

Acknowledgement

We thank Paul Arakawa of American Magnetics, Inc. for parameters values for AMI vapor-cooled leads rated at 25 kA and 40 kA. And one of authors (H. M. Kim) would like to thank Korea Science & Engineering Foundation (KOSEF) for its financial support during his stay at MIT, USA.

References

- [1] John R. Hull, High-temperature superconducting current leads, *IEEE Trans. Appl. Supercond.* **3**, 869 (1993).
- [2] Yukikazu Iwasa, "Method for current sharing in a superconducting current lead," U.S. Patent # 6,389,685 (May 21, 2002).
- [3] Yukikazu Iwasa and Haigun Lee, "High-temperature superconducting current lead incorporating operation in the current-sharing mode," *Cryogenics* **40**, 209 (2000).
- [4] Haigun Lee, Paul Arakawa, K. R. Efferson, R. Fielden, and Y. Iwasa, "AMI-MIT 1-KA leads with High-Temperature Superconducting Section – Design Concept and Key Parameters–", *IEEE Trans. on Applied Superconductivity*, Vol. 11, No. 1, March, p.2539 (2001).
- [5] Yukikazu Iwasa Case Studies in Superconducting Magnets (Plenum Press, New York, 1994).
- [6] A.F. Clark, G.E. Childs, and G.H. Wallace, "Electrical resistivity of some engineering alloys at low temperatures," *Cryogenics* **10**, 295 (1970).
- [7] Paul Arakawa (American Magnetics, Inc., private communication, 2002).
- [8] Ag/Au Thermal conductivity data paper

Haigun Lee



He was born in Chuncheon, Kangweon province, Korea. He received the B.S. degree in Materials Sci. & Eng. from Korea University, Seoul, Korea in 1987. He received the M.S. and the Ph.D degree in Materials Sci. & Eng. from University of Illinois,

Chicago in 1990 and 1995, respectively. In 1990, he entered the Third Military Academy, Korea and he was appointed with the second lieutenant in 1991. From 1995-1997, he was a postdoctoral research associate at Francis Bitter Magnet Laboratory, Massachusetts Institute of Technology (MIT).

Ho Min Kim



He was born in Jeju-city, Jeju province, Korea. He received the B.S. degree in Electrical Engineering from Cheju National University, Jeju, Korea in 1995. He received the M.S. and the Ph.D degree in Electrical Engineering from Yonsei University,

Seoul, Korea in 1998 and 2002, respectively. he is currently a postdoctoral research associate at Francis Bitter Magnet Laboratory, Massachusetts Institute of Technology (MIT).

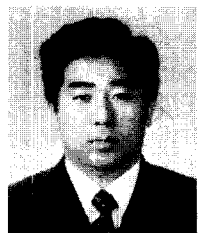
Yukikazu Iwasa



He was born in Kyoto, Japan. He received S.B and S.M. degrees in Mechanical Engineering and an S.M. degree in Electrical Engineering in 1962; an E.E. degree in Electrical Engineering in 1964; and a Ph.D. degree in Electrical Engineering in

1967, all from the Massachusetts Institute of Technology, Cambridge, MA. Except during a 1-year period 1966-1967 when he was a graduate student, he has been at the Francis Bitter Magnet Laboratory since 1964 specializing in superconducting magnet technology and cryogenic engineering. Currently he is Head of the Magnet Technology Division and research professor at FBML.

KeeMan Kim



He was born in Seoul, Korea, on November 18, 1960. He received the B.S. and the M.S. degree in nuclear engineering from Seoul national university, Seoul, Korea, in 1983 and 1985, and the Ph.D degree in nuclear engineering from University of

Illinois at Urbana-Champaign, in 1989, respectively. During 1990-1994, he was a research at Argon National Laboratory (ANL), where he was involved in the R&D on large-scale magnet applications such as linear accelerator and tokamak. In 1994, he left ANL to join the Samsung Heavy Industries, where he had a responsibility for the development of the KSTAR CICC superconducting magnet. During 1996-2002, he moved to Samsung Electronics, where he had continuously worked for the development of the KSTAR magnet, and its test facility. He is currently working at Korea Basic Science Institute as a principal researcher for the development of KSTAR devices.